


# Paradigm for approaching the forbidden phase transition in the one-dimensional Ising model at fixed finite temperature: Single chain in a magnetic field

Weiguo Yin <sup>\*</sup>

Condensed Matter Physics and Materials Science Division, Brookhaven National Laboratory, Upton, New York 11973, USA



(Received 18 December 2023; accepted 29 May 2024; published 10 June 2024)

In a previous paper [Weiguo Yin, *Phys. Rev. Res.* **6**, 013331 (2024)], the forbidden spontaneous phase transition in the one-dimensional Ising model was found to be approachable arbitrarily closely in decorated ladders by ultranarrow phase crossover (UNPC) at a given finite temperature  $T_0$  with the crossover width  $2\delta T$  reduced exponentially, which resembles a genuine first-order transition with large latent heat. Here, I reveal that the forbidden phase transition can be approached at fixed  $T_0$  as well in decorated single-chain Ising models in the presence of a magnetic field, in which  $T_0$  is determined by the interactions involving only the decorated parts and the magnetic field, while  $2\delta T$  is independently, exponentially reduced ( $\delta T = 0$  means a genuine transition) by restoring the ferromagnetic interaction between the ordinary spins on the chain backbone—which was neglected in the previous studies of pseudotransition—thus manifesting that this asymptoticity to the forbidden transition is essentially the buildup of coherence in preformed crossover of local states. Furthermore, I show that the UNPC can be realized even in the absence of the conventional geometric frustration because the magnetic field itself can induce previously unnoticed hidden spin frustration. These findings make the doors wide open to the engineering and utilization of UNPC as a new paradigm for exploring exotic phenomena and 1D device applications.

DOI: [10.1103/PhysRevB.109.214413](https://doi.org/10.1103/PhysRevB.109.214413)

## I. INTRODUCTION

The textbook Ising model describes collective behaviors such as phase transitions and critical phenomena in various physical, biological, economical, and social systems [1–4]. Since Ernst Ising’s proof one century ago [5], it has been well known that phase transition at finite temperature does not exist in the Ising model with short-range interactions in one dimension [6]. Yet, little is known about whether this forbidden transition could be approached arbitrarily closely—at fixed finite temperature  $T_0$ —until recently such asymptoticity was successfully found in decorated ladder Ising models in the absence of a magnetic field [7,8]. On the other hand, in the presence of a magnetic field, ultranarrow phase crossover termed as “pseudotransition” was found in decorated single-chain Ising models with strong geometric frustration [9–20]; however, there is no hint to the question of how to make the crossover width  $2\delta T$  narrower and narrower while keeping  $T_0$  unchanged, since  $2\delta T$  was not even defined in terms of the model parameters. The independent control of  $T_0$  and  $2\delta T$  by different interactions will not only help push the limit in our understanding of phase transitions arbitrarily close to the forbidden regime, but also provide promising potentials in technology applications. It is thus imperative to explore whether and how the forbidden in-field phase transition could be approached arbitrarily closely at a given  $T_0$  in the single-chain Ising models.

The one-dimensional (1D) Ising model on a decorated single chain is generally defined as  $H = H_{\text{ordinary}} + \sum_i H_{\text{decorated}}^{(i)}$ ,

where

$$H_{\text{ordinary}} = -J \sum_{i=1}^N \sigma_i \sigma_{i+1} - h \mu_a \sum_{i=1}^N \sigma_i \quad (1)$$

describes the ordinary single chain without the decoration [Fig. 1(a)] with  $\sigma_i = \pm 1$  standing for the  $i$ th ordinary spin—in fact, it can be used to describe any two-value system, e.g., open or close in neural networks [21], yes or no in voting.  $N$  is the total number of the ordinary spins and  $\sigma_{N+1} \equiv \sigma_1$  (i.e., the periodic boundary condition).  $J$  is the interaction between nearest-neighboring ordinary spins.  $h$  depicts the magnetic field and  $\mu_a$  the magnetic moment of the ordinary spins.  $H_{\text{decorated}}^{(i)}$  describes the decorated part in between the  $i$ th and  $(i+1)$ th ordinary spins [Fig. 1(b)], which can be any finite-size subsystem as long as it couples to the two nearest ordinary spins by the Ising-type interactions only. To date, the simplest  $H_{\text{decorated}}^{(i)}$  considered in the literature of “pseudotransition” is the Ising diamond [20] [Fig. 1(d)] given by

$$H_{\text{decorated}}^{(i)} = -J_1(\sigma_i + \sigma_{i+1}) \sum_{k=1,2} s_{i,k} - J_2 s_{i,1} s_{i,2} - h \mu_b \sum_{k=1,2} s_{i,k}, \quad (2)$$

where  $s_{i,k} = \pm 1$  denotes the  $k$ th decorated Ising spin for the  $i$ th bond of the ordinary chain or the backbone.  $\mu_b$  is the magnetic moment of the decorated spins. The antiferromagnetic  $J_1 < 0$  and  $J_2 < 0$  were considered; they form triangles yielding strong geometric frustration [22,23] near  $J_2/J_1 = 2$  [20].

<sup>\*</sup>Contact author: wyin@bnl.gov

It is instrumental to start with a comparative review of (i) the previous studies of the decorated Ising chains with pseudotransition in the presence of magnetic field [9–20] and (ii) the recent investigations of the decorated Ising ladders in the absence of the magnetic field [7,8,24]. In particular, we ask questions as to what the pseudotransition research has done and has not done, compared with what we have learned from the spontaneous ultranarrow phase crossover in the ladder. This task is greatly simplified by a recent summary [19] of the pseudotransition research in the effective Hamiltonian approach, where tracing out the decorated parts results in the ordinary Ising-chain model with temperature-dependent parameters  $J_{\text{eff}}(T)$  and  $h_{\text{eff}}(T)$  in place of  $J$  and  $h$  in Eq. (1). Two key conclusions about the existence of the pseudotransition were reached [19]: (i)  $h_{\text{eff}}(T)$  must experience the sign change as a function of temperature  $T$  and  $T_0$  is determined by  $h_{\text{eff}}(T) = 0$ . (ii) The decoration was done to create geometrical frustration so that the system's first low-lying excited state has much higher degeneracy and just slightly higher energy than the ground state, then an entropy-driven crossover between them would occur at finite temperature [9–20]. This physics of phase crossover is rather generic [23]. To make the crossover ultranarrow, it is of normal practice to place the system close to the critical point or the phase boundary in the zero-temperature phase diagram. It was found that  $T_0 \rightarrow 0$  as the pseudotransition is “tracked down in the critical point of the standard Ising-chain model at  $h = 0$  and  $T = 0$ ” [19]. In other words,

$$T_0 \rightarrow 0 \text{ as } 2\delta T \rightarrow 0, \quad (3)$$

in this traditional paradigm of realizing the ultranarrow phase crossover by approaching the zero-temperature phase boundary of two competing phases. Therefore, the pseudotransition does not appear to support our goal of approaching the forbidden phase transition at fixed finite  $T_0$ . Now that the knowledge of how to realize the goal in the Ising ladders has become available [7,8], we understand that the following key pieces of information were missing in the previous studies of pseudotransition and we are able to quickly find the solution in the term of “coherent pseudotransition” (CPT) that unifies the ultranarrow phase crossovers in both the ladder and the single-chain Ising models:

(i) *On the description of the targeted phenomenon.* The crossover width  $2\delta T$  was never clearly defined and expressed by the model parameters (note that  $\delta T = 0$  means a genuine phase transition) for the pseudotransition, while it was always presented in terms of specific heat, entropy, magnetic susceptibility, or overall magnetization [9–20]; these physical quantities are derivatives of the free energy with respect to the global parameter  $T$  or  $h$  and thus depend on the details of the model. For spontaneous CPT in decorated Ising ladders, the on-rung parent-spin correlation function was identified as the order parameter (OP) that has a well-defined value space of  $[-1, 1]$  with the value 0 meaning  $T_0$  and its inverse slope at  $T_0$  meaning  $\delta T$ , characterizing the CPT as an abrupt change in the OP between nearly  $-1$  to nearly  $+1$  [7,8]. Moreover, the general form of the OP does not depend on the details of the model; its mathematical derivation and numerical computation can be easily carried out. Such an OP provides an accurate, convenient, and microscopic description of the CPT;

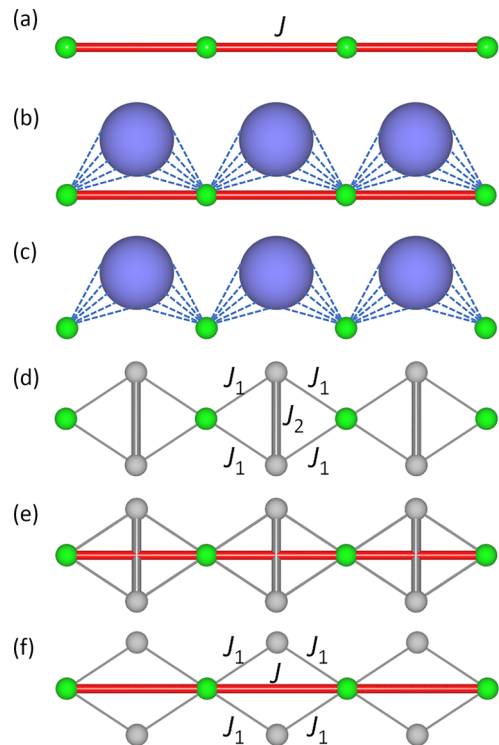


FIG. 1. Schematic diagrams of decorated Ising chains. (a) The original ordinary Ising chain [5], which consists of the Ising spins (green balls) with the ferromagnetic interaction  $J > 0$  (red bonds). (b) The decoration consists of arbitrary finite-size sublattices (big blue balls) which are coupled to the ordinary chain by the Ising-type interactions (dotted lines). (c) Decorated Ising chain with the  $J$  bonds neglected [9–20]. (d) The Ising diamond chain for  $J = 0$  [16,20], in which the decorated Ising spins (grey balls) utilize the antiferromagnetic interactions  $J_1 < 0$  and  $J_2 < 0$  (grey bonds) to form triangles, yielding geometric frustration. (e) The Ising diamond chain with ferromagnetic  $J > 0$  studied here. (f) The Ising diamond chain without geometric frustration for  $J_2 = 0$ .

its identification greatly accelerated the search for CPT. Here for the decorated single-chain Ising models, the OP that has the same features is  $\langle \sigma_i \rangle$ , the magnetization of the ordinary spins on the chain backbone (not the overall magnetization that includes the decorated parts): Its sign change and zero value at  $T_0$  is consistent with the behavior of  $h_{\text{eff}}(T)$ ; its inverse derivative at  $T_0$  defines  $\delta T = |\partial \langle \sigma_i \rangle / \partial T|_{T=T_0}^{-1}$  [Fig. 5(a)].

(ii) *On the model Hamiltonian.* Surprisingly, the  $J$  term—the Ising interaction between the ordinary spins on the chain backbone [red bonds in Figs. 1(a), 1(b), 1(e), and 1(f)]—was neglected in the previous studies of pseudotransition [9–20], that is, Fig. 1(c) was studied instead of the more general Fig. 1(b). A possible reason for the omission of  $J$  could be that the standard geometric frustration from the triangles formed by the antiferromagnetic bonds is more obvious for  $J = 0$ , as shown in Fig. 1(d) for the Ising diamond chain, the hitherto simplest model with pseudotransition. However, the CPT for the Ising ladders tells us that the on-leg decoration (which controls  $\delta T$ ) can be done independently of the on-rung decoration (which controls  $T_0$ ) [7,8]. We shall use the  $J \neq 0$  Ising diamond chain model [Fig. 1(e)] to show that similarly, the  $J$  term independently exponentially reduces the crossover width

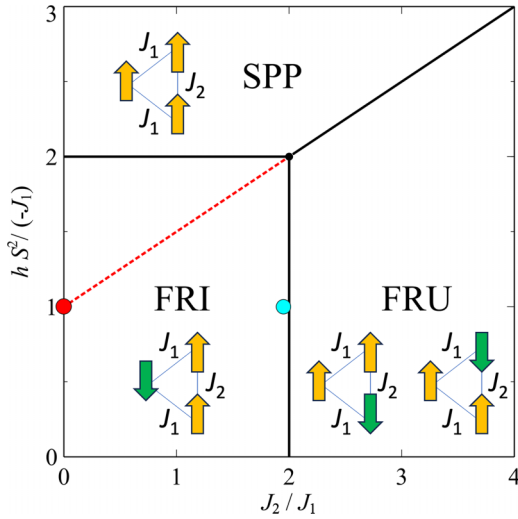


FIG. 2. The ground-state phase diagram of the Ising diamond chain in the  $J_2/J_1 - h/J_1$  plane. Following Ref. [20], we use the same notation for individual ground states to facilitate the comparison: FRI - the ferrimagnetic phase, FRU - the frustrated phase, SPP - the saturated paramagnetic phase. The focus of Ref. [20] was the case with strong geometric frustration (the cyan circle for  $J_2/J_1 = 1.95$  near the FRI – FRU boundary) as the FRU phase has the degeneracy of two per unit cell. Here we also study the case without geometric frustration (the red circle for  $J_2 = 0$ ), which is located deep in the FRI phase, far away from the other two phases, but right on the extended line of the FRU – SPP boundary (red dashed line) implying a *hidden* excited state with remarkably higher degeneracy than the FRI ground state.  $J_1 = -S^2$  and  $\mu_a = \mu_b = S$  where  $S = 1/2$ .

$2\delta T$  for fixed finite  $T_0$ , since  $J$  has no effect on  $h_{\text{eff}}(T)$  but is a separate addend in  $J_{\text{eff}}(T)$ , i.e.,  $J_{\text{eff}}(T, J) = J + J_{\text{eff}}(T, 0)$  (see Eq. (A9) in the Methods).

(iii) *On the underlying mechanism.* Only the frustration of geometric frustration type (namely the lattice has frustration regardless of the presence or absence of the magnetic field) was considered for the pseudotransition. It was recently emphasized [25] that the magnetic field on its own could induce hidden spin frustration in ferrimagnetlike systems without geometric frustration [26]. Here we show the existence of CPT in the Ising diamond chain for  $J_2 = 0$  [Fig. 1(f)], where the triangles formed by the  $J$  and  $J_1$  bonds are not frustrated because  $J > 0$  is ferromagnetic. The hidden high degeneracy generated by the magnetic field, not by geometric frustration, is explained in the ground-state phase diagram of the Ising diamond chain (the red circle on the red dashed line in Fig. 2). An immediate improvement is the dramatic increase in  $T_0$ , e.g., by 2200% when  $J_2/J_1$  is moved away from 1.95 to 0 (note that  $J_2/J_1 = 2$  sets the phase boundary), as shown in Fig. 3(b) and Figs. 4(b) and 4(d).

These findings thoroughly expose the mathematical structure of CPT as a generic mechanism for generating ultranarrow phase crossover at fixed  $T_0$  in the 1D Ising models. One can use various decorations to yield even very broad phase crossovers and then use interactions that enhance the coherence of the order parameter to turn the broad phase crossover to be the CPT—that is how CPT (coherent pseudotransition) got its name—reminiscent of the notion of preformed pairs and their coherence buildup in the field of high-temperature superconductivity [27]. Given the physical effects that the CPT resembles a genuine first-order phase transition with large latent heat and the fact that the Ising model has already been implemented in electronic circuits [28], optical networks [29], and optical lattices [30], the CPT-based 1D devices for thermal applications appear to be feasible. The features that  $T_0$  and  $2\delta T$  can be independently controlled by different parameters and different decoration methods could be attractive in engineering 1D thermal sensors, for example. The doors to the engineering and utilization of CPT are now wide open.

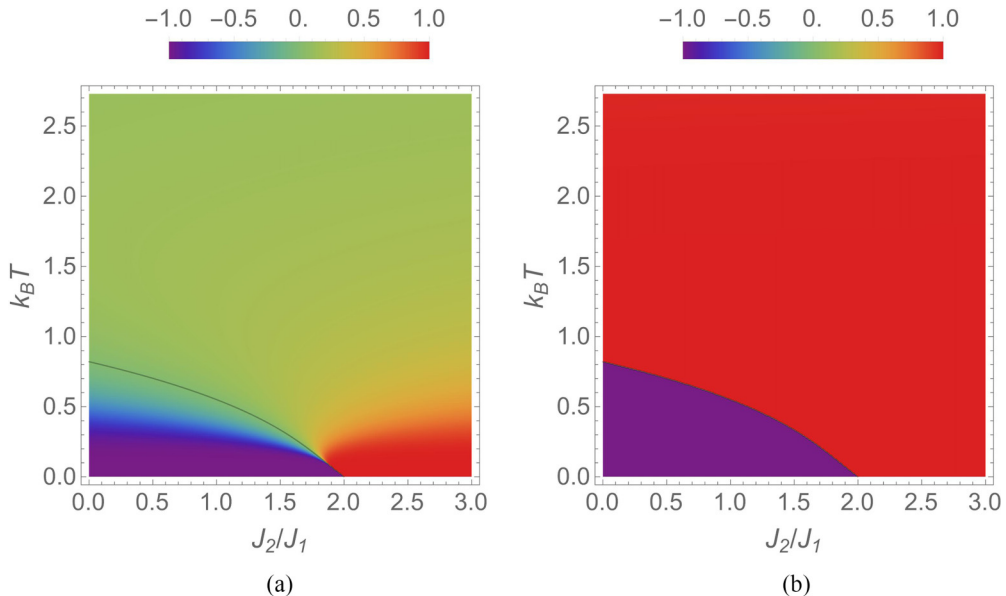


FIG. 3. The  $T - J_2$  Phase diagrams from the density plot of the order parameter  $\langle \sigma_i \rangle$  for (a)  $J = 0$  and (b)  $J = 20S^2$ . The black line is the phase boundary where  $\langle \sigma_i \rangle = 0$ .  $J_1 = -S^2$ ,  $h = 1$ , and  $\mu_a = \mu_b = S$  where  $S = 1/2$ .

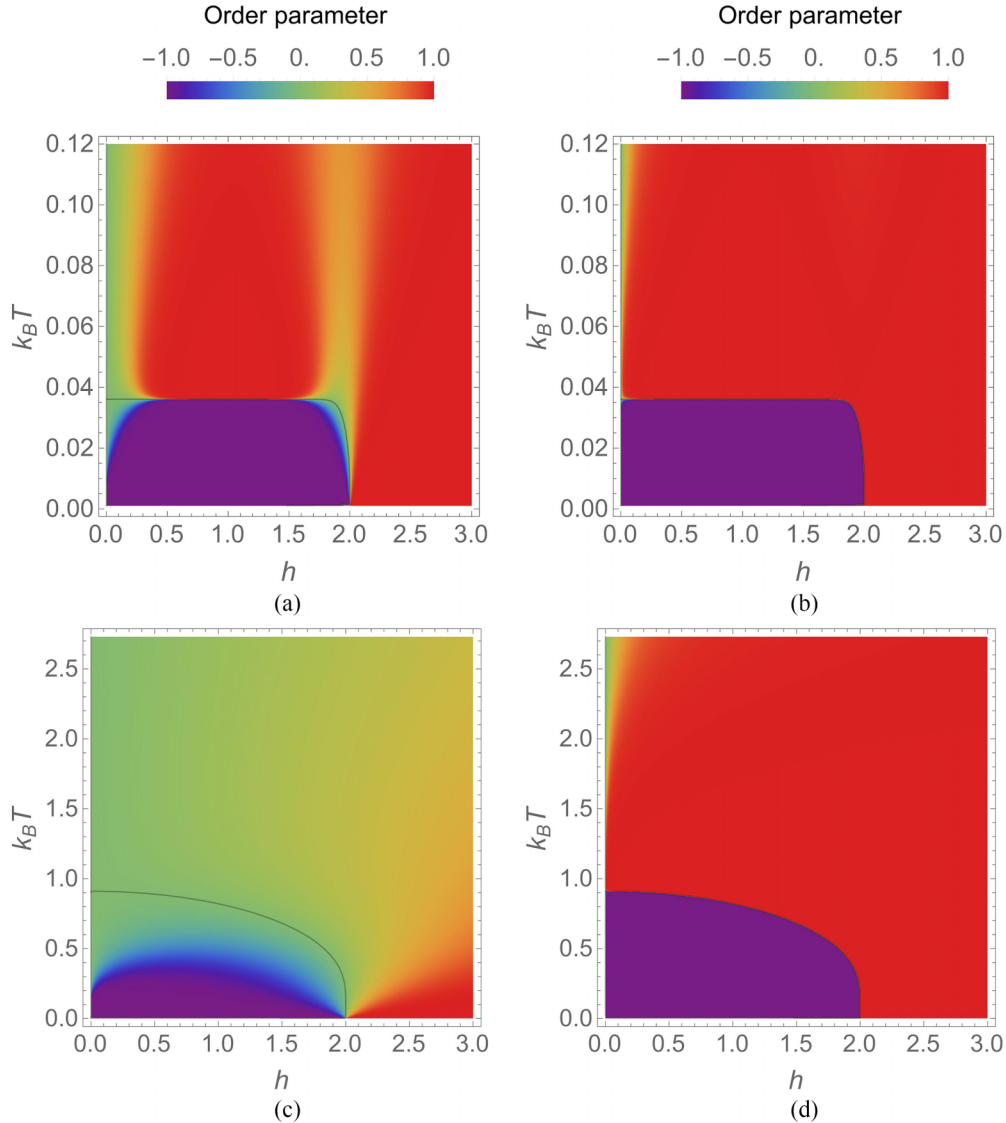


FIG. 4. The  $T - h$  Phase diagrams from the density plot of the order parameter  $\langle \sigma_i \rangle$  for (a)  $J_2/J_1 = 1.95$  and  $J = 0$ , (b)  $J_2/J_1 = 1.95$  and  $J = 0.4S^2$ , (c)  $J_2/J_1 = 0$  and  $J = 0$ , and (d)  $J_2/J_1 = 0$  and  $J = 20S^2$ . The black line is the phase boundary where  $\langle \sigma_i \rangle = 0$ .  $J_1 = -S^2$  and  $\mu_a = \mu_b = S$  where  $S = 1/2$ .

## II. RESULTS AND DISCUSSIONS

We describe the mathematical details in the Method section and show key results below. The OP is given by

$$\langle \sigma_i \rangle = \frac{\sinh(\beta h_{\text{eff}} \mu_a)}{\sqrt{\sinh^2(\beta h_{\text{eff}} \mu_a) + e^{-4\beta J_{\text{eff}}}}}. \quad (4)$$

Clearly,  $\langle \sigma_i \rangle \in [-1, 1]$ .  $\langle \sigma_i \rangle = 0$  when  $h_{\text{eff}} = 0$  at  $T_0$  and for fixed  $T_0$ ,  $\delta T \propto e^{-2J_{\text{eff}}/k_B T_0}$  exponentially decays as  $J$ , an addend in  $J_{\text{eff}}$ , increases.

The  $T - J_2$  phase diagrams from the density plot of  $\langle \sigma_i \rangle$  for the previously studied model (i.e.,  $J_2/J_1 = 1.95$  and  $J = 0$ ) [16,20] is presented in Fig. 3(a). For  $J = 0$ , the sharp phase crossover from  $\langle \sigma_i \rangle = -1$  to  $+1$  occurs only near the small region with strong geometric frustration ( $J_2/J_1 = 2$  is the FRI-FRU phase boundary; cf. Fig. 2). The resultant  $T_0$  is very low, e.g.,  $k_B T_0 S^2 / |J_1| \approx 0.036$  for  $J_2/J_1 = 1.95$  [c.f., Eq. (3)]. As  $J_2/J_1$  decreases,  $T_0$  increases ( $k_B T_0 S^2 / |J_1| \approx 0.821$  for  $J_2 = 0$ ) while the density is spread over a wider

temperature interval, meaning larger  $\delta T$ . However, for the present new model with  $J > 0$ , Fig. 3(b) shows that all the broad crossovers have been turned to be ultranarrow by increasing  $J$ . The same is observed in the  $T - h$  phase diagrams presented in Figs. 4(a) and 4(b) for  $J_2/J_1 = 1.95$  and Figs. 4(c) and 4(d) for  $J_2/J_1 = 0$ .

To gain more insights, we present the  $T$  dependence of  $h_{\text{eff}}$  and  $J_{\text{eff}}$  in Figs. 5(b) and 5(d), respectively, for  $J = 0$  and several  $J_2/J_1$ , as well as  $T_0$  and  $\delta T$  as a function of  $J_2/J_1$  in Fig. 5(c). When  $J = 0$ ,  $J_{\text{eff}}/k_B T_0 \approx 6.58$  for  $J_2/J_1 = 1.95$  resulting in  $\delta T \approx 2 \times 10^{-7}$ , but the value quickly drops to  $J_{\text{eff}}/k_B T_0 \approx 0.13$  for  $J_2 = 0$  resulting in  $\delta T \approx 1.53$ . Nevertheless, as we turn on  $J$ ,  $\delta T$  can be made narrower and narrower not only for the  $J_2/J_1 = 1.95$  already ultranarrow case [Fig. 5(e)] but also for the initially wide crossover for  $J_2 = 0$  [Fig. 5(f)] with  $T_0$  fixed in both cases. However, the underlying microscopic mechanisms for the former case with strong geometric frustration and the latter case without geometric frustration are quite different, as elaborated below.

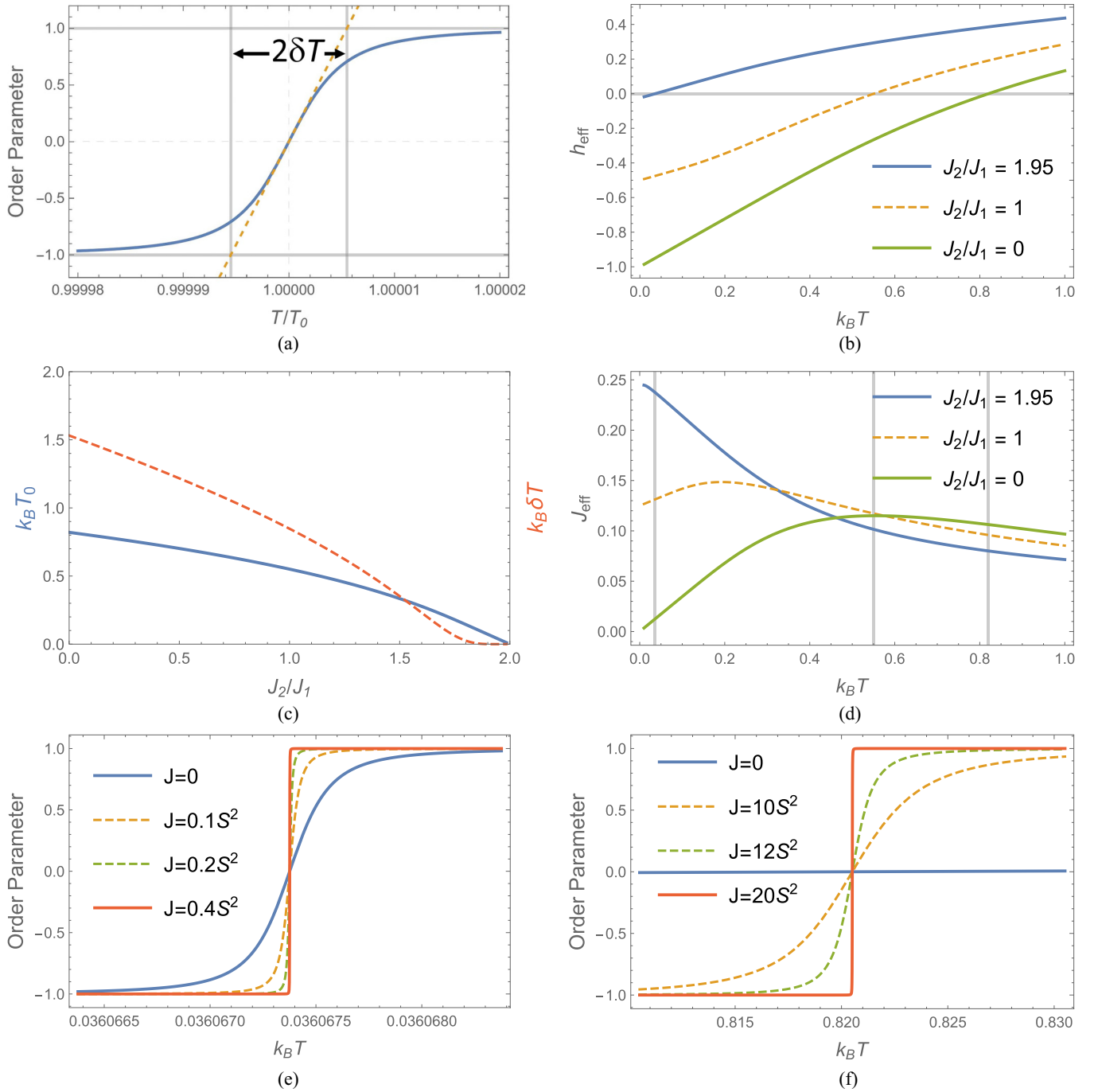


FIG. 5. Order parameter  $\langle \sigma_i \rangle$ . (a) The definition of the crossover width  $2\delta T = 2(\partial \langle \sigma_i \rangle / \partial T)_{T=T_0}^{-1}$ . The  $T$  dependence of (b)  $h_{\text{eff}}$  and (d)  $J_{\text{eff}}$  for  $J = 0$  (light gray grid lines mark where  $T_0$  is for  $J_2/J_1 = 1.95, 1, 0$ ). (c) The  $J_2/J_1$  dependence of  $T_0$  (blue solid line; left axis) and  $\delta T$  (red dashed line; right axis) for  $J = 0$ . (e) The order parameter as a function of  $T$  for  $J_2/J_1 = 1.95$ . (f) The order parameter as a function of  $T$  for  $J_2 = 0$ .  $J_1 = -S^2$ ,  $h = 1$ , and  $\mu_a = \mu_b = S$  where  $S = 1/2$ .

As shown in Fig. 6, both cases resemble a genuine first-order phase transition with the entropy jump and gigantic susceptibility at  $T_0$ , but the entropy per unit cell is flattened at  $\ln 2$  and  $2 \ln 2$  for  $J_2/J_1 = 1.95$  [Fig. 6(a)] and  $J_2 = 0$  [Fig. 6(b)], respectively. The former is expected since the case with  $J_2/J_1 = 1.95$  is located near the FRI-FRU phase boundary in the ground-state phase diagram (the cyan circle in Fig. 2). The FRU phase has the degeneracy of two per unit cell due to the frustrated decorated spins; the crossover

is driven by this entropy gain by  $\ln 2$  per unit cell [20], while the ordinary spins flip from  $\sigma_i \approx -1$  to  $+1$ , still being locked together by large  $J_{\text{eff}}/k_B T_0$ . By sharp contrast, the case with  $J_2 = 0$  is far away from any phase boundary and the entropy flattening at  $2 \ln 2$  is astonishing. This exotic phenomenon originates from a hidden remarkably high degeneracy induced by the magnetic field even in the system without geometric frustration: As shown by the red circle in Fig. 2, the case with  $J_2 = 0$  is seated right on the extended line of the



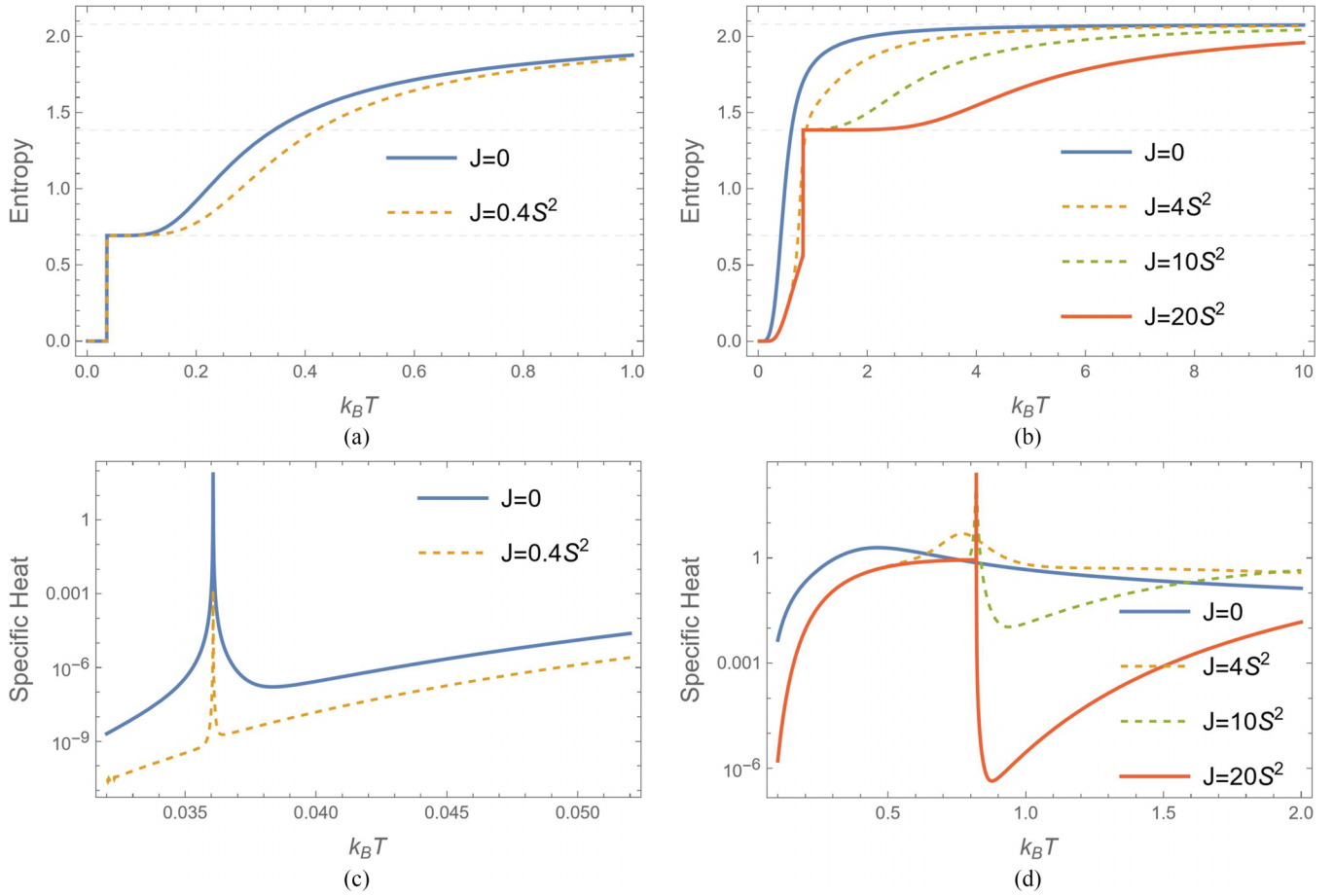


FIG. 6. Thermodynamic properties. Entropy for (a)  $J_2/J_1 = 1.95$  and (b)  $J_2/J_1 = 0$ , where the three light gray dashed lines denote the values of  $\ln 2$ ,  $2 \ln 2$ , and  $3 \ln 2$ . Specific heat for (c)  $J_2/J_1 = 1.95$  and (d)  $J_2/J_1 = 0$ .  $J_1 = -S^2$ ,  $h = 1$ , and  $\mu_a = \mu_b = S$  where  $S = 1/2$ .

FRU-SPP phase boundary (red dashed line). This means that once the system is heated out of the FRI ground state, it will be frustrated in choosing between FRU or SPP, resulting in the effective decoupling of the two decorated spins per unit cell from the lattice—that is the entropy gain of  $2 \ln 2$ . Meanwhile, the ordinary spins flip from  $\sigma_i \approx -1$  to  $+1$  and are still locked together by large  $J_{\text{eff}}/k_B T_0$ . In other words, it is this lockup, “calm,” or the buildup of coherence in the order parameter  $\sigma_i$  of the ordinary spins that makes the decorated spins fully frustrated in response to the heated atmosphere. This is a distinctly new mechanism for driving the CPT. It is also opposite to the zero-temperature critical point recently emphasized as the “half-ice half-fire” state in ferrimagnetlike systems where the ordinary spins are fully frustrated while the decorated spins are forced to be calm by the critical magnetic field [25]. Now the FRI regime of the ground-state phase diagram has two paths toward CPT through either the geometric-frustration-driven FRI-FRU or the hidden-frustration-driven FRU-SPP phase boundary. As demonstrated in the density plot of the entropy right above  $T_0$  [Fig. 7(a)] and that of the entropy jump at  $T_0$  [Fig. 7(b)], the entropy jump of about  $\ln 2$  to  $2 \ln 2$  takes place in most areas of the FRI regime except for weak  $h$  and the largest jump occurs approximately along the hidden frustration line. This difference in the entropy jump together with  $T_0$  and  $\delta T$  could be used to train deep neural networks to predict the model parameters of the decorated 1D Ising model with CPT [31].

### III. SUMMARY

In summary, a simple and general way of including the ferromagnetic  $J$  term is found to not only transform all the previously studied systems—with geometric frustration—in the context of pseudotransition into the ultranarrow phase crossover that possesses the highly desirable features:  $T_0$  and  $2\delta T$  can be independently controlled by different parameters and different decoration methods, but also unexpectedly expose the hidden field-induced frustration to generate the ultranarrow phase crossover in decorated Ising chains without the conventional geometric frustration. With the discoveries of both the spontaneous ultranarrow phase crossover in the decorated Ising two-leg ladders (which is DNA-like) and the field-driven ultranarrow phase crossover in the decorated Ising single chains (which is RNA-like), the foundation of the research direction in ultranarrow phase crossover has been solidly established. Given the prominent roles of the Ising model and frustration in understanding collective phenomena in various physical, biological, economical, and social systems, and the prominent roles of 1D systems in research, education, and technology applications, as well as the recent technological advancement that the Ising model has already been implemented in various physical systems [28–30], we anticipate that the present new insights to phase transitions and frustration effects will stimulate further research

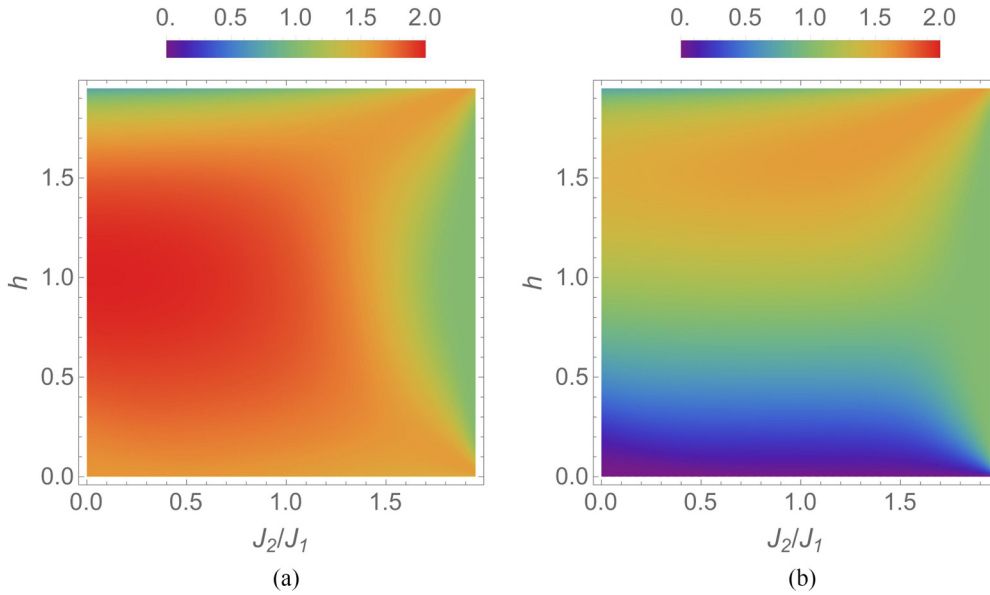


FIG. 7. The  $h - J_2$  density plots of (a) the entropy right above  $T_0$  and (b) the entropy jump at  $T_0$  in the unit of  $\ln 2$  per unit cell.  $J = 20S^2$ ,  $J_1 = -S^2$ , and  $\mu_a = \mu_b = S$  where  $S = 1/2$ .

and development about ultranarrow phase crossover and its applications.

#### ACKNOWLEDGMENTS

The author is grateful to D.C. Mattis for mailing him a copy of Ref. [1] as a gift and inspiring discussions over the years. Brookhaven National Laboratory was supported by U.S. Department of Energy (DOE) Office of Basic Energy Sciences (BES) Division of Materials Sciences and Engineering under contract No. DE-SC0012704.

The author declares no competing interests.

#### APPENDIX A: THE METHOD

The central quantity of statistic mechanics is the partition function  $Z = \text{Tr}(e^{-\beta H})$  where  $H$  is the Hamiltonian of the system and  $\beta = 1/(k_B T)$  with  $T$  being the temperature and  $k_B$  the Boltzmann constant [1]. The free energy per unit cell  $f(T) = -\frac{1}{N} k_B T \ln Z$  (where  $N$  is the number of unit cells) determines many important thermodynamic properties such as the entropy  $S = -\partial f / \partial T$ , the specific heat  $C_v = T \partial S / \partial T$ , the magnetization  $m = -\partial f / \partial h$ , and the magnetic susceptibility  $\chi = \partial m / \partial h$ . Here the OP is  $\langle \sigma_i \rangle = -(1/h) \partial f / \partial \mu_a$ .

The partition function of a 1D Ising model can be obtained exactly by using the transfer matrix method [1-4,7-20,25,26] and is given by

$$Z = \text{Tr}(\Lambda^N) = \sum_k \lambda_k^N \rightarrow \lambda^N \quad \text{for } N \rightarrow \infty, \quad (\text{A1})$$

where  $\Lambda$  is the transfer matrix,  $\lambda_k$  the  $k$ th eigenvalue of  $\Lambda$ , and  $\lambda$  the largest eigenvalue. Thus, in the thermodynamic limit, the free energy per unit cell  $f(T) = -\lim_{N \rightarrow \infty} \frac{1}{N} k_B T \ln Z = -k_B T \ln \lambda$ .

To calculate the partition function  $Z = \text{Tr}(e^{-\beta H})$  for the general model of the decorated Ising chains defined in Eq. (1)

and illustrated in Fig. 1(b), the decorated sites can be exactly summed out as they are coupled only to the nearest neighboring ordinary spins, yielding *the decoration's contribution functions*

$$\boxed{\pm\pm}_i = \sum (e^{\beta H_{\text{decorated}}^{(i)}})_{\sigma_i = \pm 1, \sigma_{i+1} = \pm 1} \quad (\text{A2})$$

where the sum is over all possible states made up by the decorated subsystem for one of the four combinations of  $(\sigma_i, \sigma_{i+1}) = (\pm 1, \pm 1)$ . They are translationally invariant, i.e.,  $\boxed{\pm\pm}_i = \boxed{\pm\pm}$ .

The transfer matrix is of the following form:

$$\Lambda_{\text{single-chain}} = \begin{pmatrix} a & c \\ c & b \end{pmatrix} = \begin{pmatrix} e^{\beta J + \beta h \mu_a} \boxed{++} & e^{-\beta J} \boxed{+-} \\ e^{-\beta J} \boxed{-+} & e^{\beta J - \beta h \mu_a} \boxed{--} \end{pmatrix}, \quad (\text{A3})$$

Its largest eigenvalue is

$$\lambda = \frac{1}{2} e^{\beta J} [\Upsilon_+ + \sqrt{\Upsilon_-^2 + 4e^{-4\beta J} \boxed{+-}}], \quad (\text{A4})$$

with *the frustration functions*

$$\Upsilon_{\pm} = e^{\beta \mu_a h} \boxed{++} \pm e^{-\beta \mu_a h} \boxed{--}, \quad (\text{A5})$$

which is independent of  $J$ .

The crossing of  $a$  and  $b$  in Eq. (A3) occurs when  $\Upsilon_-$  changes sign at  $T_0$  where  $\Upsilon_- = 0$ . **This means that  $T_0$  is independent of  $J$ .** Meanwhile, the  $\boxed{+-}$  term in Eq. (A4) has a prefactor of  $e^{-4\beta J}$ , **which exponentially decreases to zero as ferromagnetic  $J > 0$  increases for fixed finite  $T_0$** ; thus, if Eq. (A4) is approximated by neglecting the  $\boxed{+-}$  term inside  $\sqrt{\dots}$ ,

$$\lambda \simeq \frac{1}{2} e^{\beta J} (\Upsilon_+ + |\Upsilon_-|), \quad (\text{A6})$$

which becomes non-analytic. The difference between Eq. (A4) and Eq. (A6) takes place in a region of  $(T_0 - \delta T, T_0 + \delta T)$ , where the crossover width  $\delta T$  can be estimated by  $|\Upsilon_-| = 2e^{-2\beta J} \boxed{+-}$  at  $T_0 \pm \delta T$ . Following Ref. [7], an alternative and consistent way to measure  $\delta T$  is to find such an order parameter that has a well-defined value space of  $[-1, 1]$  with the value 0 meaning  $T_0$  and its inverse slope at  $T_0$  meaning  $\delta T$ . It is the magnetization of the ordinary spins given by

$$\langle \sigma_i \rangle = -\frac{\partial f}{h \partial \mu_a} = \frac{\Upsilon_-}{\sqrt{\Upsilon_-^2 + 4e^{-4\beta J} \boxed{+-}^2}}. \quad (\text{A7})$$

$$\delta T = \left( \frac{\partial \langle \sigma_i \rangle}{\partial T} \right)_{T=T_0}^{-1} = e^{-\frac{2J}{k_B T_0}} \frac{4k_B T_0^2 \boxed{+-}}{-\Upsilon_+} \left[ 2h\mu_a + \left( \frac{\partial \ln \boxed{++}}{\partial \beta} - \frac{\partial \ln \boxed{--}}{\partial \beta} \right) \right]_{\beta=\frac{1}{k_B T_0}}^{-1}. \quad (\text{A8})$$

Again, it is clear that the crossover width  $\delta T$  decreases exponentially as  $J$  increases for fixed finite  $T_0$ . This order parameter provides an accurate, convenient, and microscopic description of CPT. The use of the CPT order parameter accelerates the finding of CPT.

The above exact solution can also be represented in terms of temperature-dependent effective interactions and field on the ordinary spins [7,8,19,24]:

$$\begin{aligned} h_{\text{eff}} &= \frac{1}{2\beta\mu_a} (\ln a - \ln b) = h + \frac{1}{2\beta\mu_a} (\ln \boxed{++} - \ln \boxed{--}), \\ J_{\text{eff}} &= \frac{1}{2\beta} \left[ \frac{1}{2} (\ln a + \ln b) - \ln c \right] = J + \frac{1}{2\beta} \left[ \frac{1}{2} (\ln \boxed{++} + \ln \boxed{--}) - \ln \boxed{+-} \right], \\ A &= \frac{1}{2\beta} \left[ \frac{1}{2} (\ln a + \ln b) + \ln c \right] = \frac{1}{2\beta} \left[ \frac{1}{2} (\ln \boxed{++} + \ln \boxed{--}) + \ln \boxed{+-} \right]. \end{aligned} \quad (\text{A9})$$

Note that  $\mu_a$  appears in  $h_{\text{eff}}$  only and  $J$  appears in  $J_{\text{eff}}$  only—with  $J_{\text{eff}}(T, J) = J + J_{\text{eff}}(T, 0)$ . This means that  $J$  has no impact on the determination of  $T_0$ , therefore it can be used to change  $\delta T$  for fixed  $T_0$ . The resulting transfer matrix is expressed by

$$\Lambda_{\text{single-chain}} = \begin{pmatrix} a & c \\ c & b \end{pmatrix} = e^{\beta A} \begin{pmatrix} e^{\beta J_{\text{eff}} + \beta h_{\text{eff}} \mu_a} & e^{-\beta J_{\text{eff}}} \\ e^{-\beta J_{\text{eff}}} & e^{\beta J_{\text{eff}} - \beta h_{\text{eff}} \mu_a} \end{pmatrix}, \quad (\text{A10})$$

Its largest eigenvalue is

$$\lambda = e^{\beta A} e^{\beta J_{\text{eff}}} [\cosh(\beta h_{\text{eff}} \mu_a) + \sqrt{\sinh^2(\beta h_{\text{eff}} \mu_a) + e^{-4\beta J_{\text{eff}}}}]. \quad (\text{A11})$$

$T_0$  is determined by  $\sinh(\beta h_{\text{eff}} \mu_a) = 0$ , i.e.,  $h_{\text{eff}}(T_0) = 0$  [19], which is the same as  $\Upsilon_-(T_0) = 0$ . The order parameter is

$$\langle \sigma_i \rangle = -\frac{\partial f}{\partial (h\mu_a)} = -\frac{\partial f}{\partial (h_{\text{eff}} \mu_a)} = \frac{\sinh(\beta h_{\text{eff}} \mu_a)}{\sqrt{\sinh^2(\beta h_{\text{eff}} \mu_a) + e^{-4\beta J_{\text{eff}}}}}. \quad (\text{A12})$$

$$\delta T = \left( \frac{\partial \langle \sigma_i \rangle}{\partial T} \right)_{T=T_0}^{-1} = e^{-\frac{2J_{\text{eff}}}{k_B T_0}} \frac{k_B T_0^2}{-\cosh(\beta h_{\text{eff}} \mu_a)} \left[ h_{\text{eff}} \mu_a + \beta \mu_a \left( \frac{\partial h_{\text{eff}}}{\partial \beta} \right) \right]_{\beta=\frac{1}{k_B T_0}}^{-1}. \quad (\text{A13})$$

Eq. (A12) and Eq. (A13) are the same as Eq. (A7) and Eq. (A8), respectively. These two different representations can be used to verify the results obtained from using the other method.

For the Ising diamond chain model defined in Eq. (2) and illustrated in Fig. 1(e),

$$\begin{aligned} \boxed{++} &= 2 \cosh(4\beta J_1 + 2\beta h\mu_b) e^{\beta J_2} + 2e^{-\beta J_2}, \\ \boxed{--} &= 2 \cosh(4\beta J_1 - 2\beta h\mu_b) e^{\beta J_2} + 2e^{-\beta J_2}, \\ \boxed{+-} &= \boxed{-+} = 2 \cosh(2\beta h\mu_b) e^{\beta J_2} + 2e^{-\beta J_2}. \end{aligned} \quad (\text{A14})$$

For  $J_2 = 0$ , the Ising diamond chain does not have geometric frustration, as shown in Fig. 1(f),

$$\begin{aligned} \boxed{++} &= [2 \cosh(2\beta J_1 + \beta h\mu_b)]^2, \\ \boxed{--} &= [2 \cosh(2\beta J_1 - \beta h\mu_b)]^2, \\ \boxed{+-} &= \boxed{-+} = [2 \cosh(\beta h\mu_b)]^2. \end{aligned} \quad (\text{A15})$$

$$\delta T = e^{-\frac{2J}{k_B T_0}} \frac{2k_B T_0^2 \boxed{+-}}{-\Upsilon_+} [h\mu_a + (2J_1 + h\mu_b) \tanh(2\beta J_1 + \beta h\mu_b) - (2J_1 - h\mu_b) \tanh(2\beta J_1 - \beta h\mu_b)]_{\beta=\frac{1}{k_B T_0}}^{-1}. \quad (\text{A16})$$



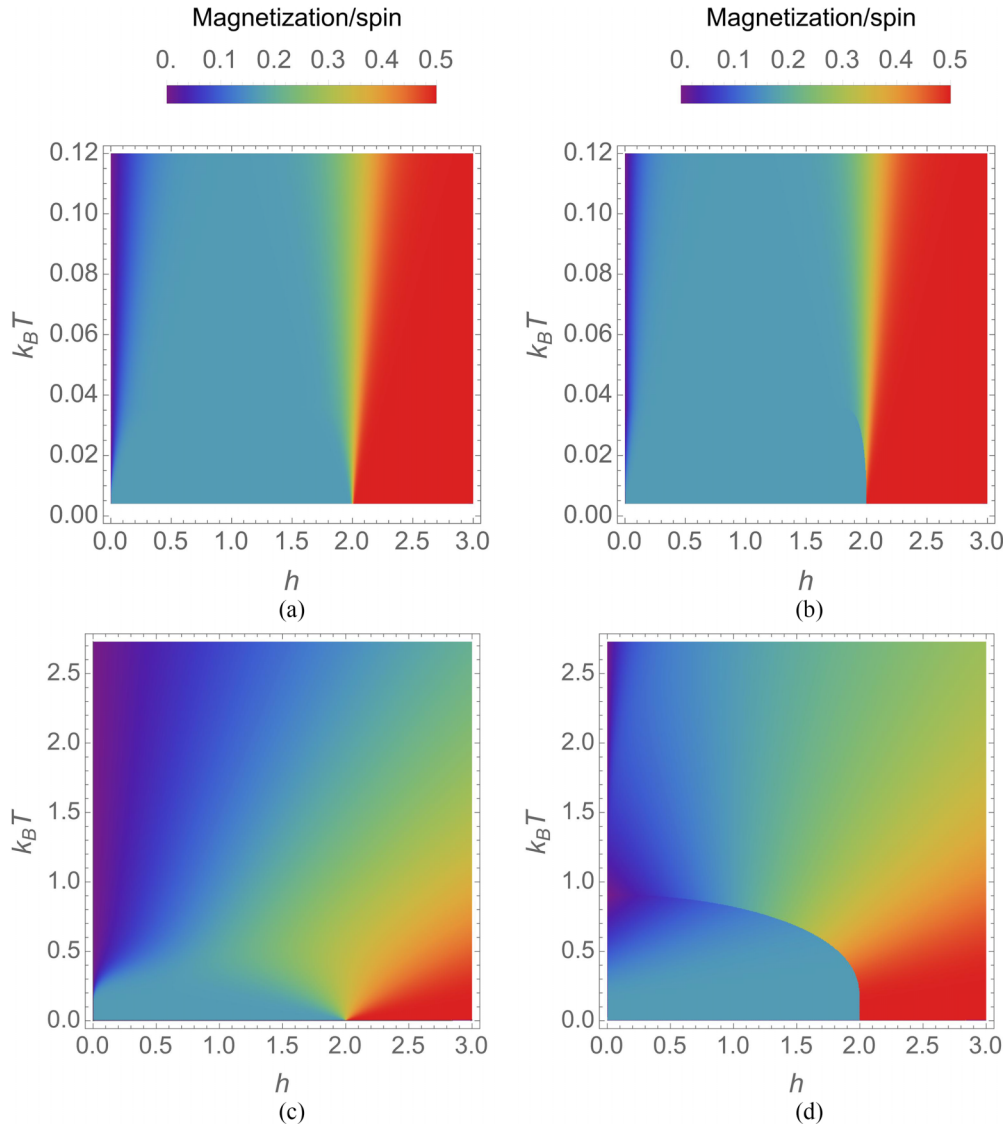


FIG. 8. The  $T - h$  Phase diagrams from the density plot of the magnetization per spin  $m/3 = (\mu_a \langle \sigma_i \rangle + \mu_b (s_{i,1} + s_{i,2}))/3$  for (a)  $J_2/J_1 = 1.95$  and  $J = 0$ , (b)  $J_2/J_1 = 1.95$  and  $J = 0.4S^2$ , (c)  $J_2/J_1 = 0$  and  $J = 0$ , and (d)  $J_2/J_1 = 0$  and  $J = 20S^2$ .  $J_1 = -S^2$  and  $\mu_a = \mu_b = S$  where  $S = 1/2$ .

To compare with the previously reported results [20], the following transformation is needed:

$$J \rightarrow JS^2, \quad J_1 \rightarrow J_1 S^2, \quad J_2 \rightarrow J_2 S^2, \quad \mu_a = \mu_b = S, \quad (\text{A17})$$

where  $S = 1/2$ , as done for all the results presented in this manuscript.

#### APPENDIX B: THE MAGNETIZATION

It is noteworthy that the magnetization  $m = \mu_a \langle \sigma_i \rangle + \mu_b \sum_k \langle s_{i,k} \rangle$  offers less clear evidence of the CPT at  $T_0$ . It was shown that for  $J_2/J_1 = 1.95$  and  $J = 0$ , no traces of the pseudo-transition could be found in the density plot of  $m$  [see

Fig. 8(a)], while the pseudo-transition could be clearly seen in the respective density plots of the entropy, susceptibility, and specific heat [20]. This insensitivity of  $m$  can be explained by the fact that  $J_2/J_1 = 1.95$  is near the FRI-FRU phase boundary where  $m$  is almost the same on both sides with exactly two spins up and one down per unit cell in the ground state as shown in Fig. 2. This feature remains unchanged for  $J > 0$  [see Fig. 8(b)]. When moving away from the FRI-FRU phase boundary,  $m$  becomes a better indicator of the CPT; for example, for  $J_2 = 0$ , the hidden frustration involves the SPP phase and the CPT can be revealed in the density plot of  $m$  except for the weak  $h$  region [see Fig. 8(d)]. The comparison between  $m$  and  $\langle \sigma_i \rangle$  the OP will be addressed in more details in subsequent publications [32].

- [1] D. C. Mattis and R. Swendsen, *Statistical Mechanics Made Simple*, 2nd ed. (World Scientific, Singapore, 2008).
- [2] D. C. Mattis, *The Theory of Magnetism II* (Springer, Berlin, Heidelberg, 1985).
- [3] R. J. Baxter, *Exactly Solved Models in Statistical Mechanics* (Academic Press, New York, 1982).
- [4] K. Huang, *Statistical Mechanics* (John Wiley & Sons, Hoboken, NJ, 2008).
- [5] E. Ising, Beitrag zur theorie des ferromagnetismus (Contribution to theory of ferromagnetism), *Z. Phys.* **31**, 253 (1925).
- [6] J. A. Cuesta and A. Sánchez, General non-existence theorem for phase transitions in one-dimensional systems with short range interactions, and physical examples of such transitions, *J. Stat. Phys.* **115**, 869 (2004).
- [7] W. Yin, Paradigm for approaching the forbidden spontaneous phase transition in the one-dimensional Ising model at a fixed finite temperature, *Phys. Rev. Res.* **6**, 013331 (2024).
- [8] W. Yin, Finding and classifying an infinite number of cases of the marginal phase transition in one-dimensional Ising models, [arXiv:2006.15087](https://arxiv.org/abs/2006.15087).
- [9] L. Gálisová and J. Strečka, Vigorous thermal excitations in a double-tetrahedral chain of localized Ising spins and mobile electrons mimic a temperature-driven first-order phase transition, *Phys. Rev. E* **91**, 022134 (2015).
- [10] J. Torrico, M. Rojas, S. de Souza, and O. Rojas, Zero temperature non-plateau magnetization and magnetocaloric effect in an Ising-XYZ diamond chain structure, *Phys. Lett. A* **380**, 3655 (2016).
- [11] S. de Souza and O. Rojas, Quasi-phases and pseudo-transitions in one-dimensional models with nearest neighbor interactions, *Solid State Commun.* **269**, 131 (2018).
- [12] I. Carvalho, J. Torrico, S. de Souza, M. Rojas, and O. Rojas, Quantum entanglement in the neighborhood of pseudo-transition for a spin-1/2 Ising-XYZ diamond chain, *J. Magn. Magn. Mater.* **465**, 323 (2018).
- [13] O. Rojas, A conjecture on the relationship between critical residual entropy and finite temperature pseudo-transitions of one-dimensional models, *Braz. J. Phys.* **50**, 675 (2020).
- [14] O. Rojas, J. Strečka, M. L. Lyra, and S. M. de Souza, Universality and quasicritical exponents of one-dimensional models displaying a quasitransition at finite temperatures, *Phys. Rev. E* **99**, 042117 (2019).
- [15] O. Rojas, J. Strečka, O. Derzhko, and S. M. de Souza, Peculiarities in pseudo-transitions of a mixed spin-(1/2, 1) Ising–Heisenberg double-tetrahedral chain in an external magnetic field, *J. Phys.: Condens. Matter* **32**, 035804 (2019).
- [16] J. Strečka, Peculiarities in pseudo-transitions of a mixed spin-(1/2, 1) Ising–Heisenberg double-tetrahedral chain in an external magnetic field, *Acta Phys. Pol. A* **137**, 610 (2020).
- [17] L. Čanová, J. Strečka, and M. Jaščur, Exact results of the Ising–Heisenberg model on the diamond chain with spin-1/2, *Czech. J. Phys.* **54**, 579 (2004).
- [18] L. Čanová, J. Strečka, and M. Jaščur, Geometric frustration in the class of exactly solvable Ising–Heisenberg diamond chains, *J. Phys.: Condens. Matter* **18**, 4967 (2006).
- [19] T. Krokhumalskii, T. Hutak, O. Rojas, S. M. de Souza, and O. Derzhko, Towards low-temperature peculiarities of thermodynamic quantities for decorated spin chains, *Physica A* **573**, 125986 (2021).
- [20] J. Strečka, Pseudo-critical behavior of spin-1/2 Ising diamond and tetrahedral chains, in *An Introduction to the Ising Model*, edited by S. Luoma (Nova Science Publishers, New York, 2020), pp. 63–86.
- [21] E. Schneidman, M. J. Berry, R. Segev, and W. Bialek, Weak pairwise correlations imply strongly correlated network states in a neural population, *Nature (London)* **440**, 1007 (2006).
- [22] L. Balents, Spin liquids in frustrated magnets, *Nature (London)* **464**, 199 (2010).
- [23] S. Miyashita, Phase transition in spin systems with various types of fluctuations, *Proc. Jpn. Acad., Ser. B* **86**, 643 (2010).
- [24] T. Hutak, T. Krokhumalskii, O. Rojas, S. Martins de Souza, and O. Derzhko, Low-temperature thermodynamics of the two-leg ladder Ising model with trimer rungs: A mystery explained, *Phys. Lett. A* **387**, 127020 (2021).
- [25] W. Yin, C. R. Roth, and A. M. Tsvelik, Spin frustration and an exotic critical point in ferromagnets from nonuniform opposite  $g$  factors, *Phys. Rev. B* **109**, 054427 (2024).
- [26] G. M. Bell, Ising ferrimagnetic models. I, *J. Phys. C* **7**, 1174 (1974).
- [27] V. J. Emery and S. A. Kivelson, Importance of phase fluctuations in superconductors with small superfluid density, *Nature (London)* **374**, 434 (1995).
- [28] F. Ortega-Zamorano, M. A. Montemurro, S. A. Cannas, J. M. Jerez, and L. Franco, Fpga hardware acceleration of Monte Carlo simulations for the Ising model, *IEEE Transactions on Parallel and Distributed Systems* **27**, 2618 (2016).
- [29] D. Pierangeli, G. Marucci, and C. Conti, Large-scale photonic Ising machine by spatial light modulation, *Phys. Rev. Lett.* **122**, 213902 (2019).
- [30] H. Bernien, S. Schwartz, A. Keesling, H. Levine, A. Omran, H. Pichler, S. Choi, A. S. Zibrov, M. Endres, M. Greiner, V. Vuletić, and M. D. Lukin, Probing many-body dynamics on a 51-atom quantum simulator, *Nature (London)* **551**, 579 (2017).
- [31] J. Lee, M. R. Carbone, and W. Yin, Machine learning the spectral function of a hole in a quantum antiferromagnet, *Phys. Rev. B* **107**, 205132 (2023).
- [32] W. Yin, Approaching the forbidden phase transition in the Ising model, III: Hidden frustration, continuous marginal phase transition, and the minimal model, [arXiv:2401.00948](https://arxiv.org/abs/2401.00948).